TURBULENT STRUCTURE OF COMBINED-CONVECTION BOUNDARY LAYER ALONG A VERTICAL HEATED PLATE

Yasuo Hattori
Hydraulics Department, Central Research Institute of Electric Power Industry (CRIEPI)
1646 Abiko, Abiko-shi, Chiba 270-1194, Japan
yhattori@criepi.denken.or.jp

Toshihiro Tsuji
Department of Mechanical Engineering, Nagoya Institute of Technology (NIT)
Gokiso-cho, Showa-ku, Nagoya 466-8555, Japan
tsuji@megw.mech.nitech.ac.jp

Yasutaka Nagano
Department of Environmental Technology, Graduate School of Engineering
Nagoya Institute of Technology (NIT)
Gokiso-cho, Showa-ku, Nagoya 466-8555, Japan
nagano@heat.mech.nitech.ac.jp

Nobukazu Tanaka
Hydraulics Department, Central Research Institute of Electric Power Industry (CRIEPI)
1646 Abiko, Abiko-shi, Chiba 270-1194, Japan
n-tanaka@criepi.denken.or.jp

ABSTRACT
The turbulent structure of a combined-convection boundary layer along a vertical isothermally-heated plate in air aided by a uniform freestream has been experimentally investigated with a particle image velocimetry. High-speed and large-scale fluid motions, which strongly generate turbulent energy, are frequently observed in the natural-convection boundary layer. On the contrary, in the combined-convection boundary layer, fluctuating velocities become small with a decrease in the scale of fluid motions as freestream velocity increases. Fluctuating velocity vectors clearly indicate that the freestream imposed at the edge of the boundary layer restrains large-scale fluid motions in the outer region. In addition, any quasi-coherent structures as observed in ordinary boundary layers do not exist in the near-wall region of the combined-convection boundary layer, which shows a significant difference of the turbulent energy production through deformation of the mean motion by Reynolds shear stress between combined and forced convection.

INTRODUCTION
For the turbulent combined-convection boundary layer with an aiding flow, it has been determined that the suppression of turbulence and the reduction in the heat transfer rate arise under certain conditions (e.g., Hall and Price, 1970; Easby, 1978; Kitamura and Inagaki, 1987; Patel et al., 1998). It is of importance to elucidate why such phenomena occur, because turbulent combined-convection flows are frequently encountered in engineering applications (Quintiere et al., 1981; Chao et al., 1983; Kraus and Bar-Cohen, 1983; Siebers, 1983; Hattori et al., 1995; Sakamoto et al., 2000).

Generally, turbulent combined convection may be classified into two categories according to the main driving force in the development of flow. One is turbulent forced convection affected by buoyancy, and it was clarified by direct numerical simulations (DNS) of channel flows (Kasagi and Nishimura, 1997) that buoyancy solely affects the mean flow field and some modification of stress balance leads to a change in the Reynolds stress distribution and a reduction in the heat transfer rate. The other is a flow created by imposing a weak aiding freestream on turbulent natural convection. However, because the turbulent combined-convection boundary layer is endowed with relatively large fluctuations of velocity and temperature at low velocity and measurements near the wall are especially difficult, only a few information on the behavior of the near-wall turbulent quantities intimately related with heat transfer characteristics were reported and many unknown parts still remain. So that, the origin of the reduction in the heat transfer rate has not been identified.

To clarify why the heat transfer rate in such a boundary layer decreases with a weak aiding freestream, we have conducted experiments and a liner stability analysis on turbulent characteristics of a combined-convection boundary layer along a vertical heated plate (Hattori et al., 1999; 2000a; 2000b; 2001). Measurements with normal hot- and cold-wires and a particle image velocimetry revealed that the state of the whole boundary layer suddenly changed with increasing freestream velocity, and the laminarization of the boundary layer was caused by the transition location to turbulence moving downstream quite rapidly. This means that the combined-convection boundary layer with an increase of aiding freestream becomes more stable.

In the present study, therefore, aiming to comprehend the stabilizing effects of freestream, the velocity fields of the turbulent natural- and combined-convection boundary layers along a vertical heated plate in air have been measured with a particle image velocimetry (PIV). The structural characteristics of the fluctuating velocity field near the wall and the effects of freestream on the large-scale fluid motions in the outer region, which play a predominant role in the turbulence generation, are scrutinized on the basis of visualized images of fluid flow. Then, an extended discussion on the changes in the mechanism of turbulent production with an introducing freestream velocity is provided.

EXPERIMENTAL APPARATUS AND PROCEDURE

The experimental apparatus comprises a vertical wind tunnel, a heated flat plate and measurement instruments (Hattori et al., 2000a). The heated plate generating a buoyant flow was a 4 m high and 0.8 m wide aluminum plate and installed vertically in the test section (1×1 m^2 in area and 6.2 m high) of the wind tunnel with solid boundaries. To provide the leading edge of the plate, the heated surface was protruded 10 mm from the wall of the test section, and the surface temperature was kept uniform by controlling the heating current of each heater with the digital indicating controllers (Chino: DB500) and thyristor regulators (Chino: JA2020N).

Since the stability of boundary layers strongly depended on the magnitude of disturbances immanent in the freestream, four fine-mesh damping screens and a honeycomb were installed in the settling chamber (2×2 m^2 in area and 1 m long) placed upstream of the contraction cone to reduce the freestream disturbances. For the pure forced-convection boundary layer, the boundary layer transition from laminar to turbulence occurred at the Reynolds number of approximately 3.5×10^5.

The instantaneous two-dimensional velocity fields in the streamwise-transverse (x-y) and streamwise-spanwise (x-z) planes were measured with a PIV. Plastic microspheres of about 30 μm in diameter (Japan Fillite: EXPANCEL461DE) were added to the boundary layer flow as tracer particles and illuminated by Laser light sheets formed with a double pulse YAG Laser (New Wave Research: DPIV-N90-30) and sheet-forming optical lens. Visualized flow images were captured by a CCD camera (Sony: XC-003), and the NTSC image-outputs were recorded on a laser disc (Sony: CRV-3000AN) at 30 frames per second. Through a frame grabber, the NTSC composite signals were converted to digitized images of 512×480 pixels in size and 8 bit gray level, and each digital TV frame was separated into two digital TV fields. Velocity vectors were calculated with a pattern cross-correlation method. The local particle-image displacement was determined from interrogation windows with a size of 24×24 pixels, and 3,600 velocity vectors were obtained in each frame. Then, for determining mean and turbulent statistics, fluctuating velocity vectors in excess of 3.5 times the standard deviation from the mean value were eliminated as erroneous vectors. The mean value and standard deviation were obtained by using all velocity vectors (150,000 vectors per point).

For constant local Grashof number, Grx = 2.0×10^{11}, experiments were conducted at two different local Reynolds numbers, Rex = 0 (freestream velocity U_∞ = 0 m/s, Grx/Rex = ∞) and 4.5×10^4 (U_∞ = 0.28 m/s, Grx/Rex = 4.4×10^6), considering the fact that the laminarization of the boundary layer arises at Grx/Rex = 3×10^6 (Hattori et al., 2001). The uniform surface temperature T_w and the ambient fluid temperature T_∞ were 92 ℃ and 12 ℃, respectively. The vertical distance x from the leading edge of the flat plate to the measuring location was 2.965 m. Physical properties were evaluated at the film temperature $T_f = (T_w + T_\infty) / 2$ except for the coefficient of volume expansion β.

RESULTS AND DISCUSSION

Basic turbulent statistics

For the natural-convection boundary layer, the streamwise mean velocity U, the intensities of streamwise and transverse fluctuating velocities, u and v, and the Reynolds shear stress $\overline{uv}$ normalized by the maximum mean velocity U_m are shown in Figs. 1 and 2, compared with hot-wire measurements (Tsuji and Nagano, 1988b). Because the local Grashof number in the present experiment is quite different from that in the measurement with hot-wire, the distance from the wall is normalized by the integral thickness of the velocity boundary layer defined by the follow equation:

$$\delta_u = \int_0^\infty (U/U_m)dy$$

These coordinates are suitable for scaling the flow field in the outer region of the turbulent natural-convection boundary layer (Tsuji and Nagano, 1989). As seen in Figs. 1 and 2, the profiles of the turbulent statistics measured with PIV generally agree with hot-wire measurements. Especially, for the streamwise mean velocity U and the intensities of u and v, the PIV results almost coincide with hot-wire data (Tsuji and Nagano, 1988a). However, the Reynolds shear stress $\overline{uv}$ obtained with PIV tends to be slightly smaller than that of Tsuji and Nagano (1988b). This discrepancy may be attribute to differences in the experimental conditions such as the local Grashof number and the gradient of ambient temperature in the vertical direction (Tsuji and Nagano, 1988a). Moreover, for PIV, it is feared that the peak-locking vectors and error vectors cause measurement errors. By examining the frequency spectra of measured fluctuating velocities, only low frequency fluctuations below 10 Hz were judged to be reliable, and thus the PIV was adequate only for the observation of large-scale fluid motions.

The intensity profiles of transverse fluctuating velocity v and the Reynolds shear stress $\overline{uv}$ normalized by the maximum mean velocity U_m for the turbulent natural- and combined-convection boundary layers are plotted in Fig. 3 against the dimensionless distance from the wall $\eta = (y/x)\ \mathrm{Gr}x^{1/4}$ (Hattori et al., 2000). In the natural-convection boundary layer, the maximum intensity of v occurs beyond the maximum mean velocity location ($\eta \simeq$ 3). The Reynolds shear stress also takes the maximum value at almost the same location in the outer region as the maximum intensity of v. On the other hand, for the combined-convection boundary layer, the intensity of fluctuating velocity and the Reynolds shear stress decrease, though the appearances of each profile are similar to those of natural convection. It should be noted that, despite the increase in the mean velocity gradient near the wall, $\overline{uv}$ of combined convection becomes positive at the maximum mean velocity location and almost zero near the wall. Tsuji and Nagano (1988a, 1988b, 1992) confirmed through their experiments that the near-wall turbulence structures of natural convection significantly differ from those of forced convection. Thus, such a profile of $\overline{uv}$ measured with PIV may suggest that the peculiar structure also exists in the combined-convection boundary layer.

Structural characteristics of velocity field in near-wall region

For the combined-convection boundary layer ($\mathrm{Gr}x = 2.0\times10^{11}$ and $\mathrm{Re}x = 4.5\times10^{4}$), the instantaneous fluctuating velocity vectors and the gray level plot of instantaneous values of Reynolds shear stress uv in the (x-y) plane (80×80 mm^2 in area) are demonstrated in Fig. 4. Here, the fluctuating velocities were determined by subtracting time-averaged velocities from instantaneous ones (Reynolds decomposition). Signals of u and v, suggesting intermittent bursts as observed in the forced-convection boundary layer, could not be recognized for the turbulent combined-convection boundary layer, and the invasion of low-speed fluid (u < 0 and v < 0) frequently appeared even in the near-wall region where the mean velocity gradient takes a positive value. Such low-speed fluid motions may be a dominant cause of the peculiar $\overline{uv}$ profile measured near the wall, because the instantaneous value of Reynolds shear stress uv becomes positive. Then, these low-speed fluid motions yield a strong velocity gradient line inclined at 40 degrees to the wall, and the maximum velocity location approaches to the wall. Thus, the high correlation between uv and velocity gradient occurs instantaneously.

The instantaneous vectors consisting of fluctuating velocities u and w observed at the near-wall location η = 1.16 (y = 5.0 mm) and the gray level plot of instantaneous u value are presented in

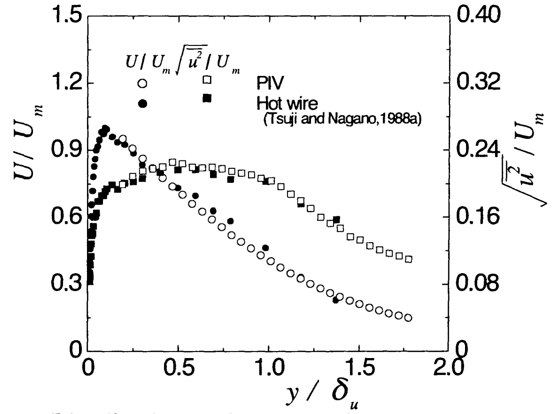

Fig. 1 Distributions of streamwise mean velocity and intensity of streamwise fluctuating velocity in natural-convection boundary layer

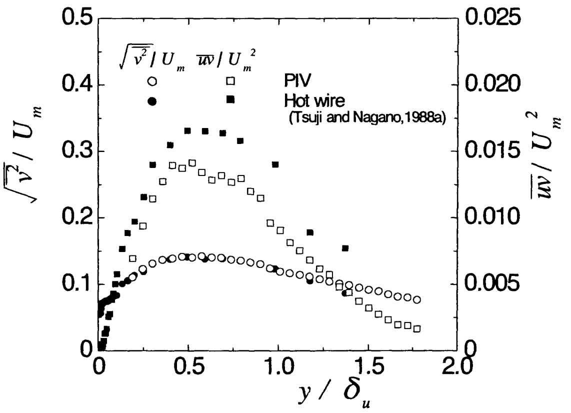

Fig. 2 Distributions of transverse fluctuating velocity and Reynolds shear stress in natural-convection boundary layer

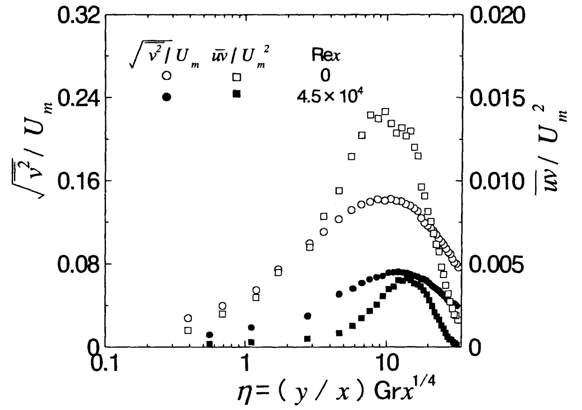

Fig. 3 Comparison of distributions of turbulent statistics between natural- and combined-convection boundary layers

Fig. 5. The visualized images are 210×210 mm^2 in area and the fluctuating velocities u and w are defined as the differences between instantaneous velocities and the mean values of the whole instantaneous velocities in the (x-z) plane. For the fluctuating velocity field depicted in Fig. 5, the two-point spatial correlations in the z direction were calculated. Figure 6 shows the spatial correlation coefficients $R_{uu}(\Delta z)$ and $R_{ww}(\Delta z)$ for u and w fluctuations. The correlation coefficient $R_{uu}(\Delta z)$ decreases and then increases with increasing Δz, which takes an infinitesimal value at $(\Delta z/x)\mathrm{Gr}x^{1/4} = 6$. This behavior of the correlation coefficient may put in mind of the existence of low- and high-speed streaks near the wall. However, the time-averaged interval of streaks is quite larger than that observed in forced convection (Kim et al., 1987), and such large-scale structures appear both in the x and z directions. Moreover, the infinitesimal value in the $R_{ww}(\Delta z)$ distribution suggests the presence of counter-rotating vortex pairs, but the regularity of the vortex structure cannot be evidently recognized. Tsuji et al. (1992) and Tsuji and Nagano (1996) concluded through their experiments that any quasi-coherent structure such as low-speed streaks and intermittent bursts did not exist near the wall in the turbulent natural-convection boundary layer. Also in the near-wall region of the turbulent combined-convection boundary layer, conspicuous structures cannot be caught from two-point spatial correlations, though the velocity gradient near the wall becomes steeper with the increase in freestream velocity.

The above results indicate that the near-wall turbulent production through the mean shear stress significantly differs from that observed in forced convection. Therefore, it seems to be very difficult to correctly calculate turbulent statistics in the near-wall region of combined convection using existing turbulence models, and more advanced analyses will be required for predicting fluid motions in the combined-convection boundary layer.

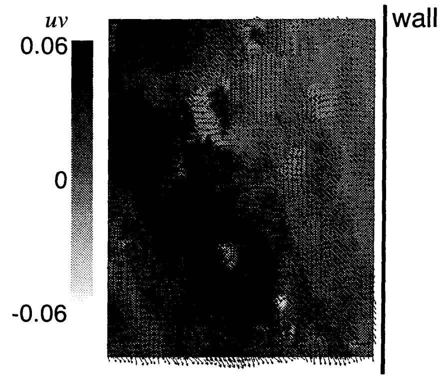

Fig. 4 Fluctuating velocity vectors with gray level plot of uv in (x-y) plane

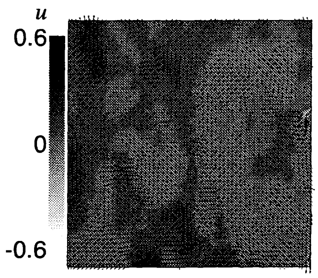

Fig. 5 Fluctuating velocity vectors with gray level plot of u in (x-z) plane

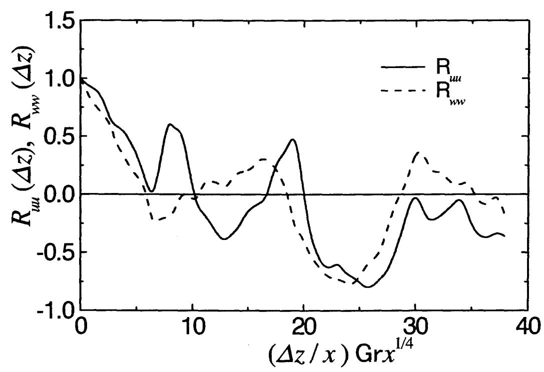

Fig. 6 Spanwise spatial correlation coefficients

Change in structures of velocity field in outer region with addition of freestream

The fluctuating velocity characteristics in the outer region of the natural- and combined-convection boundary layers have been investigated. The fluctuating velocity vectors calculated with the Reynolds decomposition in the (x-y) plane (180×180 mm^2 in area) are presented in Fig. 7. The gray levels of instantaneous value of Reynolds shear stress uv are also plotted in the figure. In the natural-convection boundary layer, high-speed and large-scale fluid motions appear in the whole outer region. Such fluid motions strongly produce turbulent energy, since uv takes a large positive value as seen in Fig. 7 and the mean velocity gradient is negative in the outer region. On the other hand, the scale of fluid motions in the combined-convection boundary layer becomes small with the reduction in the magnitude of fluctuating velocity. It is obvious that the freestream imposed at the edge of the boundary layer restrains large-scale fluid motions. Thus, the

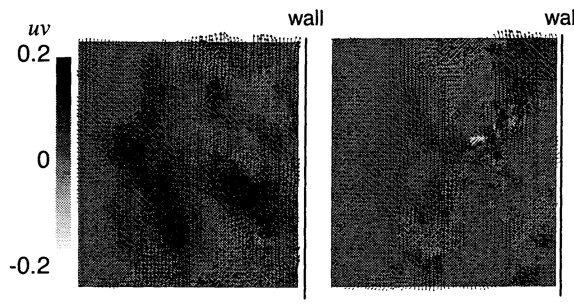

(a) $\mathrm{Re}x = 0$ (b) $\mathrm{Re}x = 4.5\times 10^4$

Fig. 7 Fluctuating velocity vectors with gray level plot of uv in (x-y) plane turbulence generation in the combined-convection boundary layer declines with changes in fluid motions, and the intensities of fluctuating velocity and the Reynolds shear stress decrease as shown in Fig. 3.

It is suggested that the choice of the reference frame is important to positively identify the vortex structure since the Reynolds decomposition often distorts the instantaneous structure and may actually mislead an exposition in some cases (Adrian, Meinhart and Tomkins, 2000). Accordingly, the reference frame appropriate to indicate structures of the fluctuating velocity field was determined by changing the convection velocity in gradual increments. The fluctuating velocity vectors, viewed in the reference frame moving at a half the maximum mean velocity, are presented in Fig. 8. Also shown in the figure is the gray level plot of streamwise fluctuating velocity u' defined as the difference between the instantaneous velocity and a half the maximum mean velocity. The fluid motions in each boundary layer are strikingly different. In the natural-convection boundary layer, non-uniform behavior of u' is notable in the x direction, and the high-speed fluid region meanders through the outer region. Simultaneously, in the x direction, the different sign of v' alternately appears near the maximum mean velocity location. The large-scale fluctuations are observed over the whole velocity field, which lead to the formation of the velocity shear layers both in the x and y directions. Such fluid motions play a predominant role in the turbulence generation, because the region of large-scale velocity fluctuations is exactly coincide with that of positive values of Reynolds shear stress uv. On the other hand, in the combined-convection boundary layer, large-scale structures in the outer region crumble due to the suppression of turbulence generation with the addition of freestream.

The fluctuating velocity vectors in the (x-z) plane (210×210 mm^2 in area) in the outer region (η = 18.0), captured for the natural- and combined-convection boundary layers, are demonstrated in Fig. 9. Here, the fluctuating velocities are again defined by subtracting spatial-averaged velocities from instantaneous ones. Large-scale fluid motions in the natural-convection boundary layer form vortexes nearly equal to those for high-speed fluid motions observed in the (x-y) plane, whereas fluid motions in the combined-convection boundary layer are quite small in scale and active fluctuations are limited to the specific region in the z direction.

Thus, the increase in freestream velocity restrains large-scale fluid motions closely related with the generation of turbulent energy in the outer region of the combined-convection boundary layer and finally causes a laminarization of the boundary layer. It is quite astonishing that the laminarization of the combined-convection boundary layer may occur even at the Grx value of 100 times as large as the critical Grashof number (Grx $\simeq$ 3×10^9) in pure natural convection, if the Rex value does not exceed the critical Reynolds number (Hattori et al., 2000).

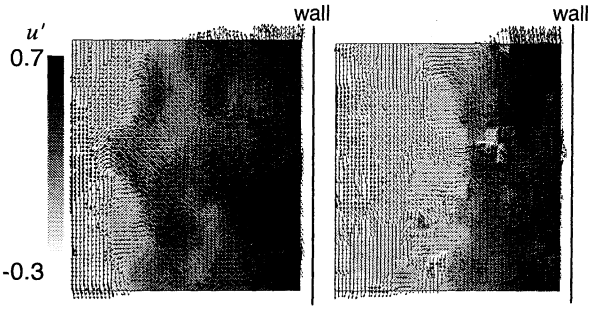

(a) Rex = 0 (b) Rex = 4.5×10^4

Fig. 8 Fluctuating velocity vectors viewed in reference frame with gray level plot of u'

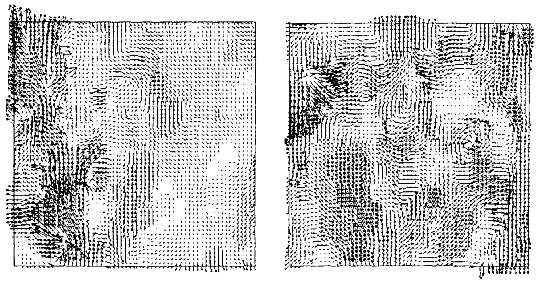

(a) Rex = 0 (b) Rex = 4.5×10^4

Fig. 9 Fluctuating velocity vectors in (x-z) plane

CONCLUDING REMARKS

The measurement with a particle image velocimetry (PIV) was conducted to investigate the turbulent structure of a combined-convection boundary layer along a vertical heated plate in air with an aiding uniform freestream. The special attention was paid to the effect of freestream on structural characteristics of the fluctuating velocity field near the wall and large-scale fluid motions in the outer region. The results of the present study may be summarized as follows.

1. For the turbulent natural-convection boundary layer, the profiles of the streamwise mean velocity U and the intensities of velocity fluctuations u and v measured with PIV generally agree well with hot-wire data. Though the Reynolds shear stress $\overline{uv}$ obtained with PIV tends to be slightly smaller than that with hot-wire, it was confirmed that the PIV is effective to examine the structural characteristics of low-speed turbulent buoyant flows.

2. Any signals of u and v, suggesting intermittent bursts as observed in the forced-convection boundary layer, could not be recognized for the turbulent combined-convection boundary layer as in the natural-convection boundary layer. The invasion of low-speed fluid (u < 0 and v < 0) is frequently observed even in the near-wall region where the

mean velocity gradient takes a positive value. Such a low-speed fluid motion may be a dominant cause of the peculiar $\overline{uv}$ profile near the wall.

3. In the natural-convection boundary layer, high speed and large-scale fluid motions, which strongly generate turbulent kinetic energy, are frequently observed. On the contrary, in the combined-convection boundary layer, the freestream imposed at the edge of the boundary layer restrains the large-scale fluid motion, and the fluctuating velocities become small with a decrease in the scale of fluid motions.

References

Adrian, R. J., Meinhart, C. D., and Tomkins, C. D., 2000. Vortexorganization in the outer region of the turbulent boundary layer. *J. Fluid Mech.* **422**, 1-54.

Chao, B. T., Chen, S. J., and Yao, L. S., 1983. Mixed convection over a vertical zircaloy plate in steam with simultaneous oxidation. *Int. J. Heat Mass Transfer* **26**, 73-82.

Easby, J. P., 1978. The effect of buoyancy on flow and heat transfer for a gas passing down a vertical pipe at low turbulent Reynolds numbers. *Int. J. Heat Mass Transfer* **21**, 791-801.

Hall, W. B., and Price, P. H., 1970. Mixed forced and free convection from a vertical heated plate to air. *Proc. 4th Int. Heat Transfer Conf.*, vol. 4, NC 3.3.

Hattori, Y., Kashiwagi, E., Yamakawa, H., and Wataru M., 1995. Experiments of natural convection to evaluate heat transfer in the spent fuel dry storage facilities. *Proc. 3rd Int. Conf. on Nuclear Engineering*, vol. 4, 1927-1932.

Hattori, Y., Tsuji, T., Nagano Y., and Tanaka, N., 1999. Characteristics of turbulent combined-convection boundary layer along a vertical heated plate, *Proc. 1st Symp. on Turbulence and Shear Flow Phenomena*, 545-550.

Hattori, Y., Tsuji, T., Nagano Y., and Tanaka, N., 2000a. Characteristics of turbulent combined-convection boundary layer along a vertical heated plate. *Int. J. Heat Fluid Flow* **21**, 520 - 525.

Hattori, Y., Tsuji, T., Nagano Y., and Tanaka, N., 2000b. Retransition from turbulence to laminar flow in a combined-convection boundary layer along a vertical heated plate, *Proc. 4th JSME-KSME Thermal Engineering Conf.*, vol. 3, 187-192.

Hattori, Y., Tsuji, T., Nagano Y., and Tanaka, N., 2001. Effects of freestream on turbulent combined-convection boundary layer along a vertical heated plate, *Int. J. Heat Fluid Flow* **22**, to be published.

Kasagi, N., and Nishimura, M., 1997. Direct numerical simulation of combined forced and natural turbulent convection in a vertical plane channel. *Int. J. Heat Fluid Flow* **13**, 88-99.

Kim, J., Moin, P., and Moser, R., 1987. Turbulence statistics in fully developed channel flow at low Reynolds number. *J. Fluid Mech.* **177**, 133-166.

Kitamura, K., and Inagaki, T., 1987. Turbulent heat and momentum transfer of combined forced and natural convection along a vertical flat plate - Aiding flow. *Int. J. Heat Mass Transfer* **30**, 23-41.

Kraus, A. D., and Bar-Cohen, A., 1983. *Thermal analysis and control of electronic equipment*, Hemisphere Pub. Corp., New York.

Patel, K. Armaly, B. F., and Chen, T. S., 1998. Transition from turbulent natural to turbulent forced convection. *ASME J. Heat Transfer* **120**, 1086-1088.

Quintiere, J. G., Rinkinen, W. J., and Jones, W. W., 1981. The effect of room openings on fire plume entrainments. *Comb. Sci. and Tech.* **26**, 193-201.

Raffel, M., Willert, C., and Kompenhans, J., 1998. *Particle image velocimetry,* Springer-Verlag, Berlin.

Sakamoto, K., Koga, T., Wataru, M., and Hattori, Y., 2000. Heat removal characteristics of vault storage system with cross flow for spent fuel, *Nuclear Engineering and Design* **195**, 57-68.

Siebers, D. L., 1983. Experimental mixed convection heat transfer from a large, vertical surface in a horizontal flow. Ph.D. thesis, Stanford University.

Tsuji, T., and Nagano, Y., 1988a. Characteristics of a turbulent natural convection boundary layer along a vertical flat plate. *Int. J. Heat Mass Transfer* **31**, 1723-1734.

Tsuji, T., and Nagano, Y., 1988b. Turbulence measurements in a natural convection boundary layer along a vertical flat plate. *Int. J. Heat Mass Transfer* **31**, 2101-2111.

Tsuji, T., and Nagano, Y., 1989. Velocity and temperature measurements in a natural convection boundary layer along a vertical flat plate. *Exp. Thermal Fluid Sci.* **2**, 208-215.

Tsuji, T., Nagano, Y., and Tagawa, M., 1992. Experiment on spatio-temporal turbulent structures of a natural convection boundary layer. *ASME J. Heat Transfer* **114**, 901-908.

Tsuji, T., and Nagano, Y., 1996. Structural characteristics of a turbulent natural convection boundary layer. *Proc. 2nd China-Japan Work Shop on Turbulent Flows*, 277-289.